AIP | APL Materials

Nature of electron correlation and hybridization in NixCu1−xMnSb Heusler alloys

I. Sarkar, S. M. Yusuf, M. Halder, A. Gloskovskii, and W. Drube

Citation: APL Mater. **4**, 086102 (2016); doi: 10.1063/1.4960389
View online: http://dx.doi.org/10.1063/1.4960389
View Table of Contents: http://scitation.aip.org/content/aip/journal/aplmater/4/8?ver=pdfcov
Published by the AIP Publishing

Nature of electron correlation and hybridization in $Ni_xCu_{1-x}MnSb$ Heusler alloys

I. Sarkar,[1,a] S. M. Yusuf,[2] M. Halder,[2] A. Gloskovskii,[1] and W. Drube[1]
[1]*DESY Photon Science, Deutsches Elektronen-Synchrotron, 22603 Hamburg, Germany*
[2]*Solid State Physics Division, Bhabha Atomic Research Centre, Mumbai 400085, India*

(Received 7 March 2016; accepted 19 July 2016; published online 4 August 2016)

The electronic structure of Heusler alloys having mixed magnetic phases, comprising of vicinal anti-ferromagnetic and ferromagnetic orders, is of great significance. We present the results of an electronic structure study on $Ni_xCu_{1-x}MnSb$ Heusler alloys, using Mn-2p core-level photoemission spectroscopy. Room temperature data in the paramagnetic phase reveal a non-monotonic variation of both electron correlation strength and conduction-band hybridization such that the former enhances while the latter weakens for compositions showing a mixed phase relative to compositions at the phase boundaries to the ordered phases. The results suggest a possible electronic driving force for settling mixed-magnetic phases.
[http://dx.doi.org/10.1063/1.4960389]

The design of half-metallic magnetic materials capable of generating spin polarized current is of immense interest both for potential device applications and fundamental understanding.[1] An ideal material for this purpose is half-Heusler alloys (HAs) made up of intermetallics of the type XYZ at 1:1:1 composition, where X and Y are transition-metals (TMs) and Z an sp-element.[2] Especially manganese(Mn)-based half-HAs became increasingly important due to highly tunable magnetic ordering[3–7] between ferromagnetic (FM) and anti-ferromagnetic (AFM) states. This tunability can be used to design mixed magnetic phases consisting of vicinal FM and AFM regions with unprecedented magnetic properties like giant exchange bias, paving way for rare earth free magneto-electronic devices.[3,4] Hence it is essential to understand what drives mixed magnetic phases in HAs from an electronic structure point of view. Here, we study the electronic structure of $Ni_xCu_{1-x}MnSb$ half-HA in the compositional range of the mixed magnetic phase by using Mn core level photoemission spectroscopy in order to understand the role of electron-electron correlations and conduction band hybridization in settling these phases.

$Ni_xCu_{1-x}MnSb$ HAs are very significant as NiMnSb (x = 1) is ferromagnetic[8] and CuMnSb (x = 0) is anti-ferromagnetic,[9] with the possibility of tuning the magnetic ordering between these two as a function of the Ni and Cu concentrations.[5–7] This versatile magnetic ordering has triggered numerous efforts to understand the evolution of magnetization from the FM to the AFM phase.[6,10] One of the most intriguing features of this evolution is the magnetic phase for Ni concentrations below x = 0.3 that shows a sudden dramatic break in the magnetization and transport properties.[6,7,10] It is assumed that for low Ni concentrations there is an onset of magnetic disorder on a structurally perfect Mn sublattice induced by chemical disorder on the Cu/Ni sublattice.[6,7] Density functional theory calculations further predict a complex magnetic phase below x = 0.2.[6,10] Although there is no clear understanding of this phase, it is proposed to arise due to competition between the two kinds of indirect exchange interactions[6,10] between Mn spins: (a) ferromagnetic Rudermann-Kittel-Kasuya-Yosida (RKKY) type exchange and (b) antiferromagnetic super-exchange. Both of these interactions strongly depend on the hybridization of Mn 3d

[a]indra7neel@gmail.com

levels with the conduction band.[10] Using neutron diffraction and neutron depolarization measurements, it has been found that for Ni concentrations between $0.05 \leq x \leq 0.2$, a mixed magnetic phase consisting of both FM and AFM regions exists at low temperature.[5]

While a number of electronic structure calculations on $Ni_xCu_{1-x}MnSb$ HAs exist,[6,10,12] especially for the magnetically ordered FM and AFM phases, an experimental study of the electronic structure for compositions showing the mixed phase has been missing. The calculations show that the magnetic properties of $Ni_xCu_{1-x}MnSb$ are determined by magnetic moments localized on Mn atoms interacting via itinerant electrons in the conduction band.[10] In the recent years, it has been shown that electronic structure calculations incorporating electron correlations are applicable to a wider class of HAs in predicting magnetic properties.[1,11] The electron correlation depends on on-site Coulomb potentials.[1] For correlated materials like HAs, electron correlation is expected to strongly affect the nature of magnetic ordering and metallicity.[1,13] Therefore, experimental electronic structure data revealing the nature of electron correlations and conduction band hybridization of HAs are extremely important for enabling the rational design of these phases.

Using high-resolution Mn-2p core-level hard X-ray photoemission spectroscopy (HAXPES), we here present an electronic structure study of $Ni_xCu_{1-x}MnSb$ for Ni concentrations x = 0.05, 0.15, and 0.2. The low and high concentrations, x = 0.05 and x = 0.2, mark the compositional boundaries of the low temperature mixed magnetic phase with the AFM and FM ordered phases.[5] Our room temperature results for the paramagnetic phase shows that in the mixed magnetic phase materials, (a) hybridization between Mn 3d levels and conduction states has a non-monotonic dependence with the variation of Ni concentration, with a minimum within the region $0.05 \leq x \leq 0.2$ and (b) the electron correlation strength is found to be higher for concentrations showing mixed magnetic phase behaviour compared to compositions corresponding to the boundaries to the ordered AFM and FM phases.

Mn 2p core level photoemission spectroscopy is a powerful probe to study electronic structure and to understand the effect of electron correlations and hybridization in Mn-based correlated materials.[14–17] This is due to the fact that during photoemission a 2p electron is emitted from Mn, leaving behind a hole in the core level. This sudden creation of a core-hole potential at the Mn site during photoexcitation initiates core hole screening which strongly depends on electron correlations and charge transfer (CT) processes. As a result, the spectral Mn 2p line shapes are characteristically modified, yielding information regarding the strength of hybridization and electron correlation in the solid.[18] Use of HAXPES in the experiment ensures that the bulk electronic structure of the HAs is probed due to the enhanced information depth.[19]

For this experiment, high quality polycrystalline $Ni_xCu_{1-x}MnSb$ (x= 0.05, 0.15, and 0.2) samples were prepared from the constituent elements with 99.99% purity by arc melting under argon atmosphere.[5] They have C_{1b} type cubic structure as shown by X-ray diffraction data,[5] such that Cu/Ni atoms occupy the sub-lattice (000) while Mn and Sb atoms occupy other the two sub-lattices (1/4 1/4 1/4) and (3/4 3/4 3/4). The fourth sublattice (1/2 1/2 1/2) is unoccupied. The measurements were carried out using the HAXPES instrument at X-ray undulator beamline P09 of PETRA III (Hamburg, Germany).[20] The photon energy was set to 5.95 keV and a grazing photon incidence angle of 5^0 relative to the sample surface was chosen. Photoelectrons emitted in the horizontal plane and normal to the sample surface were collected by a SPECS PHOIBOS 225 HV hemispherical electron energy analyzer. The exciting X-rays were monochromatized by a combination of a Si(111) double-crystal primary monochromator and a Si(333) channel-cut post-monochromator. The total energy resolution was 180 meV.[20]

Fig. 1 shows room temperature Mn 2p spectra of $Ni_xCu_{1-x}MnSb$ for varying concentrations of Ni. The spectra exhibit the typical doublet structure corresponding to Mn $2p_{3/2}$ and Mn $2p_{1/2}$ states due to spin-orbit splitting.[14] The peak separation is ≈12eV indicating strong spin-orbit coupling. The peak energy positions correspond to a Mn^{3+} valence state[22] as expected for $Ni_xCu_{(1-x)}MnSb$.[2,5] The Mn $2p_{3/2}$ peak exhibits a broad asymmetric shape along with two additional satellite features C1 and C2 on the lower and higher binding energy sides. Similar albeit weaker satellites are observed for Mn $2p_{1/2}$. The appearance of such satellite peaks in 2p core level spectra of 3d transition metal (TM) based correlated systems is well-known and related to charge transfer processes between Mn 3d and other bands related to conduction band and neighboring atoms.[14,21,22,24]

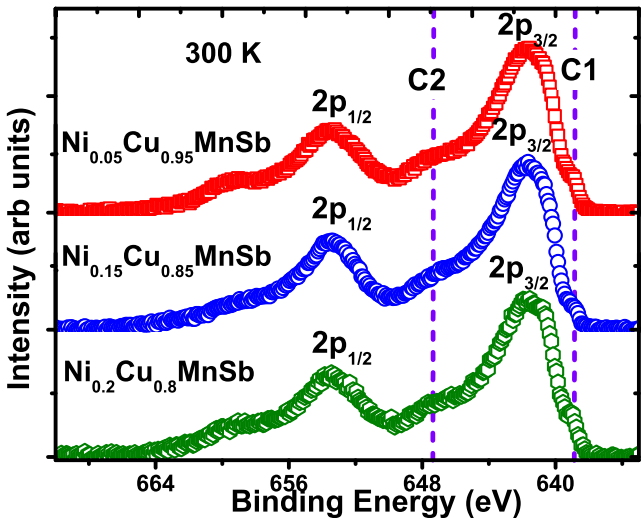

FIG. 1. Background subtracted room temperature Mn 2p spectra of $Ni_xCu_{1-x}MnSb$ for varying Ni concentrations (x = 0.05, 0.15, and 0.2). The dashed line is a guide to the eye marking structures C1 and C2 of the $2p_{3/2}$ line.

Furthermore, earlier studies have shown that the asymmetric line shapes of 2p spectra of TM can be explained within an Anderson impurity model by incorporating charge transfer to the conduction band.[21]

Temperature dependent Mn 2p spectra (Fig. 2) show that the intensity of the C1 and C2 satellites increases as the temperature is decreased. On the other hand, it is well established from electrical transport measurements on $Ni_xCu_{1-x}MnSb$ that the conductivity/metallicity increases with decreasing temperature.[7,23] Thus, the C1 and C2 satellites may be related to charge transfer between Mn 3d and metallic conduction bands at the Fermi level. Similar temperature dependent satellite structures have also been observed in Mn 2p spectra of manganites[14] as well as 2p spectra of other TMs[24] and ruthenates[25] and have been attributed to charge transfer between valence 3d states and the conduction band. Hence, the C1 and C2 satellite intensities can be viewed as a clear signature of strength of hybridization between Mn 3d and the conduction band. Appearance of C1 can be attributed to electron transfer from conduction to 3d band, while C2 to electron transfer from 3d to conduction band.[14,24] This can be understood as follows : the photoemission of a Mn 2p electron

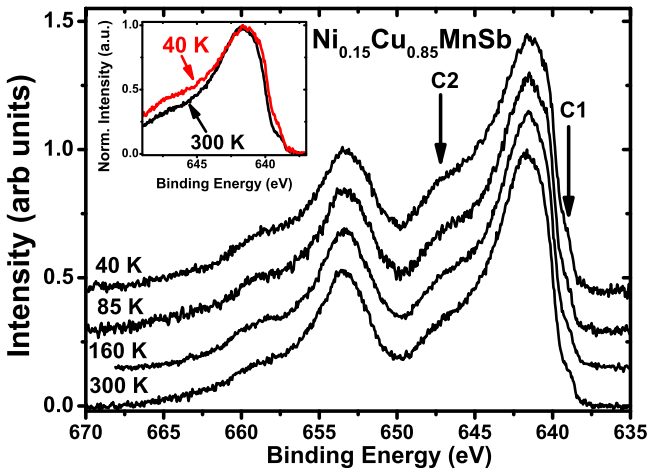

FIG. 2. Temperature dependent background subtracted Mn 2p spectra of $Ni_{0.15}Cu_{0.85}MnSb$. The inset shows spectra of $Ni_{0.15}Cu_{0.85}MnSb$ for 40 K and 300 K normalized to peak intensity. The spectra reveal enhanced C1 and C2 intensity at 40 K.

leads to a $2p^5$ final state with a core-hole. Now for a charge transfer (CT) peak for which there is an electron transfer into 3d states, there are more unpaired 3d electrons. As a result there will be enhanced core-hole repulsion between the $2p^5$ core and 3d valence states, and consequently the CT peak will appear on the lower binding energy side, as is the case for C1.[24] On the other hand, when electrons are transferred from the 3d band, the number of unpaired electron reduces and the CT peak will appear on the higher binding energy side, as observed for C2. The broader spectral width of C2 compared to C1 may be attributed to additional charge transfer from Mn 3d to neighboring atoms.[21]

The Mn 2p spectra (Fig. 1) clearly show that the intensities of the C1 and C2 satellites are reduced for x = 0.15 compared to x = 0.2 and 0.05 for the room temperature paramagnetic phase. This implies that the hybridization strength has a non-monotonic dependence on the Ni concentration. It appears to have maximum strength for concentrations near the mixed phase boundaries to the ordered FM and AFM phases. This non-monotonic dependence should have a very important consequence on the indirect exchange interaction between Mn spins. This is due to the fact that irrespective of the magnetic order in HAs being FM or AFM, both are imposed due to the indirect exchange interactions, namely ferromagnetic RKKY for the former and antiferromagnetic super-exchange for the latter. The strength of both types of exchange interaction, i.e., FM RKKY and AFM super-exchange, are proportional to the fourth power of the coupling between the Mn 3d levels and the conduction states.[10] Therefore, the present results showing weaker hybridization clearly indicate a weakening of both FM and AFM indirect exchange interactions. Such a softening of exchange interactions could be a possible driving mechanism of magnetic disorder in otherwise ordered magnetic states.

The Mn2p spectra (Fig. 3) were fitted considering charge transfer (CT) peaks and additional broadening due to final state multiplet effects (ME). ME occurs due to the non-degeneracy arising from vector coupling of angular momenta of overlapping 2p core and 3d valence wave functions.[16,18] Coupling of the $2p^5{}_{3/2}$ (j = 3/2) and $3d^4$ (J = 4) final states gives six levels with J = 11/2, 9/2, 7/2, 5/2, 3/2, 1/2, while $2p^5{}_{1/2}$ (j = 1/2) and $3d^4$ (J = 4) coupling gives five levels with J = 9/2, 7/2, 5/2, 3/2, 1/2. Therefore, including two CT peaks (C1, C2), 8 and 7 peaks were used to fit, respectively, the $2p_{3/2}$ and $2p_{1/2}$ spectra. Both the peak position and peak ratios of all ME peaks were kept constant for the different Ni concentrations. It is then found that the ME peak intensity reduces for lower J values, consistent with the atomic limit where intensities are proportional to the (2J + 1) degeneracy.[16] We note that the ME intensity ratios (Table I) for peaks well separated

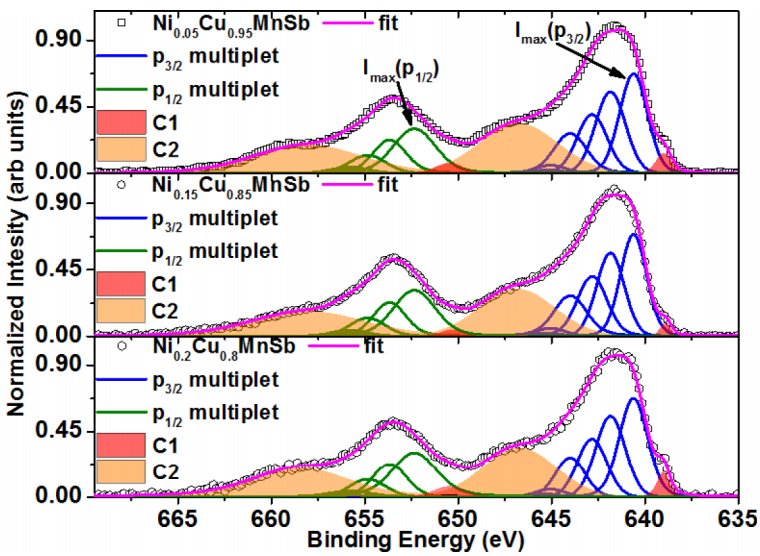

FIG. 3. Fitting of the Mn 2p spectra for varying Ni concentration, including CT and multiplet peaks. The shaded region shows CT related peaks C1 (red) and C2 (orange). Blue and green lines show the multiplet structure related to the $2p_{3/2}$ and $2p_{1/2}$ states, respectively. I_{max} denotes the highest intensity J state.

TABLE I. ME peak ratios with respect to maximum intensity $I_{max}(p_{3/2})$ and $I_{max}(p_{3/2})$ for $2p_{3/2}$ and $2p_{1/2}$ related ME peaks respectively.[a]

	$2p_{3/2}$ ME peak ratios					$2p_{1/2}$ ME peak ratios			
$\frac{I}{I_{max}}$	0.82	0.59	0.4	0.08	0.03	0.74	0.4	0.13	0.04
	(0.83)	(0.66)	(0.5)	(0.33)	(0.166)	(0.8)	(0.6)	(0.4)	(0.2)

[a]Numbers in brackets give the degeneracy ratio $(2J + 1)/(2J_{max}+1)$. $J_{max} = 11/2$ and $9/2$ for $2p_{3/2}$ and $2p_{1/2}$ related ME peaks, respectively.

from CT satellites are fairly close to the degeneracy ratio. It reduces however drastically when overlapping with CT satellites possibly indicating spectral weight transfer to CT peaks.

The CT peak parameters obtained from the fit confirm that the intensity reduces for Ni concentration x = 0.15 compared to spectra measured for x = 0.2 and 0.05 which correspond to the edge of the ordered and mixed phase. Also, the fitted results show that the CT peaks are further apart from the ME peak in case of x = 0.15 compared to x = 0.2 and x = 0.5. The effect is more pronounced for C1, as indicated by the vertical line connecting the peak positions in Figs. 4(a)-4(c). This clearly confirms the trend already seen in the measured spectra (Fig. 4(d)) showing a shift of C1 spectral weight towards lower binding energy for x = 0.15.

The fitted energy positions of the $2p_{3/2}$ related C1 peak relative to $I_{max}(p_{3/2})$ are −1.61 eV (x = 0.05), −1.74 eV (x = 0.15), and −1.64 eV (x = 0.2). This energy shift of the CT peaks relative to the main peak is a signature of the electron correlation strength.[25] This is because charge transfer leads to change in electron binding energy according to the strength of electron-electron and electron-hole coulomb potentials.[24,25] On the other hand these potentials determine the strength of electron correlation. Hence, a larger relative energy shift of the CT satellite indicates stronger electron correlation.[25] Therefore our results indicate stronger electron correlation in the middle of the compositional range showing the mixed magnetic phase. This is a very significant effect as in correlated materials, there exists a stability boundary for magnetic order depending on the strength of electron correlation.[1,26,27] If the electron correlation strength approaches this boundary, magnetic order can be suppressed.[27]

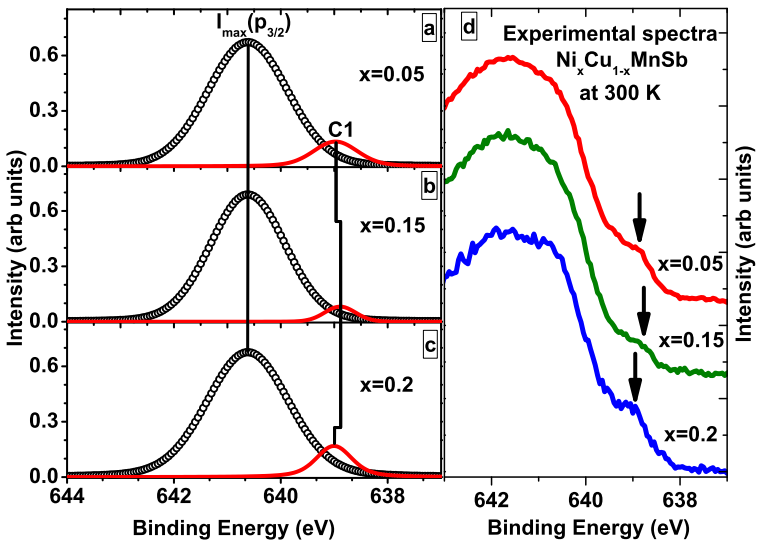

FIG. 4. $2p_{3/2}$ related I_{max} and C1 peak, obtained from fits of $Ni_xCu_{1-x}MnSb$: (a) x = 0.05, (b) x = 0.15, (c) x = 0.2. The vertical line serves as a guide to the eye joining the peak positions. The C1 peaks clearly show a larger relative peak separation for x = 0.15. (d) Experimental spectra of $Ni_xCu_{1-x}MnSb$ at 300 K with magnified region near C1 of $Mn2p_{3/2}$. The arrows mark the knee position of the C1 related part of the spectra, highlighting a spectral energy shift towards lower binding energy for x = 0.15, in accord with the fitting results.

In conclusion, we have presented results of an electronic structure study of $Ni_xCu_{1-x}MnSb$ Heusler alloys using Mn 2p photoemission spectroscopy, to reveal the nature of electron correlation and conduction band coupling with Mn 3d levels for Ni concentrations mixed magnetic phase at low temperatures. It is found primarily from room temperature data that both electron correlation and conduction band coupling vary non-monotonically with composition, such that the former reduces and the latter gains in strength at the compositional boundaries of the low temperature mixed magnetic phase materials to the ordered FM and AFM phases. As conduction band hybridization determines the strength of magnetic exchange interaction while electron correlation strength affects the stability of magnetic order, the results point to the possible electronic driving force for settling mixed magnetic phases in the Heusler alloys that are of immense importance in high spin polarized devices. The present experimental work opens an essential path for the future research that could use relative effects of electron correlation and conduction band coupling to tailor competing magnetic phases and the spin polarization in such spintronic systems.

[1] M. I. Katsnelson, V. Yu. Irkhin, L. Chioncel, A. I. Lichtenstein, and R. A. de Groot, Rev. Mod. Phys. **80**, 315 (2008).
[2] T. Graf, C. Felser, and S. S. P. Parkin, Prog. Solid State Chem. **39**, 1 (2011).
[3] A. K. Nayak, M. Nicklas, S. Chadov, P. Khuntia, C. Shekhar, A. Kalache, M. Baenitz, Y. Skourski, V. K. Guduru, A. Puri, U. Zeitler, J. M. D. Coey, and C. Felser, Nat. Mater. **14**, 679 (2015).
[4] P. Nordblad, Nat. Mater. **14**, 655 (2015).
[5] M. Halder, S. M. Yusuf, A. Kumar, A. K. Nigam, and L. Keller, Phys. Rev. B **84**, 094435 (2011).
[6] J. Kudrnovský, V. Drchal, I. Turek, and P. Weinberger, Phys. Rev. B **78**, 054441 (2008).
[7] S. K. Ren, W. Q. Zou, J. Gao, X. L. Liang, F. M. Zhang, and Y. W. Du, J. Magn. Magn. Mater. **288**, 276 (2005).
[8] R. B. Helmholdt, R. A. de Groot, F. M. Mueller, P. G. van Engen, and K. H. J. Buschow, J. Magn. Magn. Mater. **43**, 249 (1984).
[9] T. Jeong, R. Weht, and W. E. Pickett, Phys. Rev. B **71**, 184103 (2005).
[10] I. Galanakis, E. Sasioglu, and K. Özdogan, Phys. Rev. B **77**, 214417 (2008).
[11] H. C. Kandpal, G. H. Fecher, and C. Felser, J. Phys. D: Appl. Phys. **40**, 1507 (2007).
[12] E. Sasioglu, L. M. Sandratskii, and P. Bruno, Phys. Rev. B **77**, 064417 (2008).
[13] A. Garg, H. R. Krishnamurthy, and M. Randeria, Phys. Rev. Lett. **112**, 106406 (2014).
[14] K. Horiba, M. Taguchi, A. Chainani, Y. Takata, E. Ikenaga, D. Miwa, Y. Nishino, K. Tamasaku, M. Awaji, A. Takeuchi, M. Yabashi, H. Namatame, M. Taniguchi, H. Kumigashira, M. Oshima, M. Lippmaa, M. Kawasaki, H. Koinuma, K. Kobayashi, T. Ishikawa, and S. Shin, Phys. Rev. Lett. **93**, 236401 (2004).
[15] M. V. Yablonskikh, J. Braun, M. T. Kuchel, A. V. Postnikov, J. D. Denlinger, E. I. Shreder, Y. M. Yarmoshenko, M. Neumann, and A. Moewes, Phys. Rev. B **74**, 085103 (2006).
[16] P. S. Bagus, R. Broer, W. A. de Jong, W. C. Nieuwpoort, F. Parmigiani, and L. Sangaletti, Phys. Rev. Lett. **84**, 2259 (2000).
[17] S. Plogmann, T. Schlathölter, J. Braun, M. Neumann, Yu. M. Yarmoshenko, M. V. Yablonskikh, E. I. Shreder, E. Z. Kurmaev, A. Wrona, and A. Slebarski, Phys. Rev. B **60**, 6428 (1999).
[18] F. de Groot and A. Kotani, *Core Level Spectroscopy of Solids* (CRC Press, Taylor and Francis group, Florida, 2008).
[19] M. Jourdan, J. Minár, J. Braun, A. Kronenberg, S. Chadov, B. Balke, A. Gloskovskii, M. Kolbe, H. J. Elmers, G. Schönhense, H. Ebert, C. Felser, and M. Klâui, Nat. Commun. **5**, 3974 (2014).
[20] A. Gloskovskii, G. Stryganyuk, G. H. Fecher, C. Felser, S. Thieß, H. Schulz-Ritter, W. Drube, G. Berner, M. Sing, R. Claessen, and M. Yamamoto, J. Electron. Spectrosc. Relat. Phenom. **185**, 47 (2012).
[21] A. E. Bocquet, T. Mizokawa, A. Fujimori, M. Matoba, and S. Anzai, Phys. Rev. B **52**, 13838 (1995).
[22] M. C. Biesinger, B. P. Payne, A. P. Grosvenor, L. W. M. Lau, A. R. Gerson, and R. S. C. Smart, Appl. Surf. Sci. **257**, 2717 (2011).
[23] M. Halder, K. G. Suresh, M. D. Mukadam, and S. M. Yusuf, J. Magn. Magn. Mater. **374**, 75 (2015).
[24] M. Taguchi, A. Chainani, N. Kamakura, K. Horiba, Y. Takata, M. Yabashi, K. Tamasaku, Y. Nishino, D. Miwa, T. Ishikawa, S. Shin, E. Ikenaga, T. Yokoya, K. Kobayashi, T. Mochiku, K. Hirata, and K. Motoya, Phys. Rev. B **71**, 155102 (2005).
[25] H. Kim, H. Noh, K. H. Kim, and S. J. Oh, Phys. Rev. Lett. **93**, 126404 (2004).
[26] A. M. Oles and J. spalek, Z. Phys. B: Condens. Matter **44**, 177 (1981).
[27] A. M. Oles, J Phys. C: Solid State Phys. **15**, L1065 (1982).